

Structural characterization of ice polymorphs from self-avoiding walks

Carlos P. Herrero

Instituto de Ciencia de Materiales de Madrid, Consejo Superior de Investigaciones Científicas (CSIC), Campus de Cantoblanco, 28049 Madrid, Spain

(Dated: June 8, 2022)

Topological properties of crystalline ice structures are studied by means of self-avoiding walks on their H-bond networks. The number of self-avoiding walks, C_n , for eight ice polymorphs has been obtained by direct enumeration up to walk length $n = 27$. This has allowed us to determine the ‘connective constant’ or effective coordination number μ of these structures as the limit of the ratio C_n/C_{n-1} for large n . This structure-dependent parameter μ is related with other topological characteristics of ice polymorphs, such as the mean and minimum ring size, or the topological density of network sites. A correlation between the connective constant and the configurational entropy of hydrogen-disordered ice structures is discussed.

I. INTRODUCTION

Water exhibits a wide variety of solid phases, which are referred to as forms of ‘ice’. Most of these phases are produced by the application of high pressures, which yields a denser packing of water molecules than in the usual hexagonal ice Ih. Thus, sixteen different crystalline ice phases have been identified so far [1–3], and their stability range in the temperature-pressure phase diagram has been investigated for several decades. Some of their properties lack, however, a complete understanding, mainly due to their peculiar structure, where hydrogen bonds between adjacent molecules give rise to the so-called ‘water anomalies’ [1, 4, 5].

In the known ice phases except ice X, water keeps its molecular character, building up a network connected by H-bonds. In this network each water molecule is surrounded by four others, in such a way that its orientation with respect to the neighboring ones fulfills the so-called Bernal-Fowler ice rules [1, 6]. These rules allow for the presence of orientational disorder in the water molecules, which causes that in several ice phases hydrogen atoms present a disordered spatial distribution, as indicated by a fractional occupancy of their lattice sites. Thus, hexagonal ice Ih, the stable phase of solid water under normal conditions, displays hydrogen disorder compatible with the ice rules, whereas other phases such as ice II are H-ordered [7, 8].

Given the number of ice structures, a unifying classification can help to deeper understanding of their specific properties [7, 9]. For crystalline solids, classification schemes usually rest on the space symmetry, short-range atomic environments, or geometrical aspects of packing of structural units. These classification procedures have a geometrical nature, as their main criteria are geometrical characteristics of crystal structures [10–13]. These geometrical classification methods, however, can be hardly applicable to find relations between solids whose structures are somewhat distorted. A possible alternative consists in using classification schemes relying on topological criteria. This means centering attention mainly on the organization of interatomic bonds in a crystal structure as a basic criterion for a crystal-chemical analysis.

In this line, topological properties of crystalline solids have been taken into account along the years to describe properties of different types of materials [10–12]. For the ice polymorphs, a discussion of different network topologies and the relation of ring sizes in the various phases with the crystal volume was presented by Salzmann *et al.* [7]. Topological studies of three-dimensional (3D) hydrogen-bonded frameworks in organic crystals have also helped to classify this kind of structures [14]. Moreover, graph theory has been used to study isotypism and order/disorder problems in crystal structures [8, 13, 15].

A direct and rather simple topological classification of ice structures can be based on structural rings, i.e., loops of water molecules characteristic of each polymorph [7]. A more elaborate procedure can be based on the so-called ‘coordination sequence’, defined as a series of numbers $\{N_k\}$ ($k = 1, 2, \dots$), where N_k is the number of sites located at a topological distance k from a reference site [16–19]. The coordination sequence can be used to define a topological density, as a structural characteristic related to the increase in the number N_k of sites accessible through k links in a given structure [17, 20, 21]. Note that these concepts are based only on the topology of the considered network, and are not affected by lattice distortions or other structural factors. These concepts have been recently applied to ice polymorphs, allowing us to find a correlation between topological density and volume [22].

In this paper, a different way to characterize the ice polymorphs is introduced. Namely, it is based on self-avoiding walks in the corresponding structures. A self-avoiding walk (SAW) is a sequence of moves on a network that does not visit any node more than once. Contrary to unrestricted walks, SAWs contain implicit information on the topology of the considered network, as they are sensitive to characteristics such as the number and size of loops present in the structure. A particularly interesting parameter is the so-called connective constant or effective coordination number of the ice networks, which can be calculated from the long-distance behavior of the number of possible SAWs in the corresponding structures. These concepts are explained in detail in the following section.

The purpose of this paper is twofold. On one side,

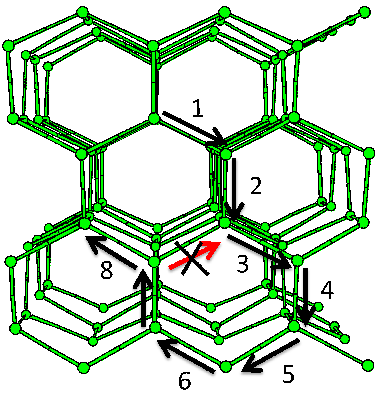


FIG. 1: Sketch of the ice Ih structure with an eight-step self-avoiding walk. A cross indicates a non-allowed step.

knowledge of the connective constants of ice structures is interesting from a basic point of view for their comparison with other crystal structures, for which this kind of statistical-mechanics questions have been analyzed in detail. On the other side, they are relevant for a topological and physico-chemical characterization of ice phases, allowing us to connect structural and thermodynamic properties of this type of solids. In particular, the configurational entropy associated to the hydrogen distribution on the available lattice sites is known to depend on the ice structure [23–25], so that a search for structural variables suitable to quantify in some way such a dependence is worthwhile in the context of ice thermodynamics.

II. COMPUTATIONAL METHOD

In order to study SAWs for the different ice polymorphs, we consider each structure as defined by the positions of the oxygen atoms. One has thus a network, where the nodes are O sites, and the links are H-bonds between nearest neighbors. The network coordination is four ($z = 4$), which gives a total of $2N$ links, N being the number of nodes. We implicitly assume that on each link there is one H atom, but its consideration is not relevant for our present purposes.

A self-avoiding walk on an ice network is defined as a walk in the simplified structure which can never intersect itself. On a given network, the walk is restricted to move to a nearest neighbor site during each step, and the self-avoiding condition constrains the walk to occupy only sites which have not been previously visited in the same walk [26–28]. We illustrate the application of this definition to ice Ih in Fig. 1, where an eight-step SAW is shown. Note that the link indicated with a cross is not available for step $n = 8$, as the walk would reach a node already visited in an earlier step.

SAWs have been used in condensed-matter science for several purposes. For instance, they were employed for modeling the large-scale properties of long-flexible

macromolecules in solution and adsorbed on surfaces [27, 29–31], as well as for the study of polymers trapped in confined regions, gel electrophoresis, and size exclusion chromatography, which deal with the transport of polymers through membranes with very small pores [32–34]. They have been also employed in the analysis of critical phenomena in lattice models [26, 35–38], and to study complex networks [39–41]. Moreover, SAWs with multiple site weightings and restrictions have been discussed in the literature [42, 43].

Given a network and a site i in it, we will call C_n^i the number of different SAWs of length n starting from this site. For networks where all sites are topologically equivalent, the sequence $\{C_n^i\}_{n=1}^{\infty}$ will coincide for all nodes, but in general, sequences corresponding to different nodes in a network may be different. (Note that for all sequences mentioned in the following n is understood to run from 1 to ∞ , although not explicitly indicated.) It is important to recall that crystallographically equivalent sites are always topologically equivalent, but sites non-equivalent crystallographically may be topologically equivalent or not [22]. Then, we define an average sequence $\{C_n\}$ for each network, where for a given n , C_n is obtained by averaging the C_n^i values for the oxygen sites in the unit cell:

$$C_n = \frac{1}{M} \sum_i m_i C_n^i. \quad (1)$$

Here m_i is the multiplicity of site i in the unit cell and $M = \sum_i m_i$. For ice structures including oxygen sites topologically non-equivalent (e.g., ices III, IV, V, VI, and XII; see Ref. [22]), relative differences between C_n^i values corresponding to different sites in a given structure decrease fast with the walk length n . In fact, the relative difference is about 1% for $n = 25$, and becomes negligible in the large- n limit.

It is remarkable that universal constants are known to describe some properties of self-avoiding walks. These constants depend on the network dimension, and have been discussed in detail in the literature [44, 45]. Other parameters controlling the long-distance behavior of SAWs are network-dependent, and can be used to characterize different networks with the same dimension. Analytical expressions describing the asymptotic behavior of SAWs for large n are significantly different from those of unrestricted walks. It is particularly interesting the dependence of C_n on the number of steps n for long walks. Its asymptotic behavior for large n is known to be given by [44–46]

$$C_n \sim n^{\gamma-1} \mu^n, \quad (2)$$

where γ is a critical exponent which takes a value $\approx 7/6$ for 3D structures [45, 47, 48], and μ is the so-called ‘connective constant’ or effective coordination number of the corresponding structure [27, 45, 46].

Defining the ratio

$$x_n = \frac{C_n}{C_{n-1}} \quad (3)$$

one has

$$x_n \approx \mu \left(1 + \frac{1}{n-1}\right)^{\gamma-1} \xrightarrow{n \rightarrow \infty} \mu \quad (4)$$

so that the (non-universal) parameter μ can be obtained as the large- n limit of the sequence $\{x_n\}$. The connective constant depends upon the particular topology of each structure, and has been determined very accurately for standard 3D lattices. In particular, for the diamond structure (with the same topology as cubic ice Ic), one has $\mu = 2.8790$ [48, 49]. In general, for structures with coordination number z , one has $\mu \leq z - 1$ [27].

For some ice networks, the convergence of x_n to the connective constant μ is rather smooth, but in other cases an odd-even alternation is present. For this reason, it is convenient to average out this effect partially by evaluating the average values

$$y_n = \frac{1}{2} (x_n + x_{n+1}) \quad (5)$$

and then studying the convergence of the sequence $\{y_n\}$ for $n \rightarrow \infty$. This is the procedure that will be employed here. We have verified that the connective constant μ so obtained from the average sequence $\{C_n\}$ coincides within error bars with that yielded by averaging the values derived independently from the sequences $\{C_n^i\}$ of different network nodes.

This procedure gives a good estimate of the connective constant, but other, more elaborate, numerical methods such as differential approximants are known to yield more accurate estimates for the extrapolated values of μ from the sequence $\{C_n\}$ [28, 50]. Such a high precision, required for some studies in statistical physics, is not necessary for our present purposes. In fact, the estimated error bar of the μ values derived from our extrapolation of the sequence $\{y_n\}$ is $\pm 2 \times 10^{-4}$. A check of this extrapolation method is provided by the ice Ic network, that is equivalent in our context to the diamond structure. The parameter μ derived here for ice Ic is consistent with the value found for diamond in earlier estimations [48, 49] (see below).

The sequence $\{C_n\}$ for a given ice structure depends only on the topology of the network, and not on the actual symmetry, cell parameters, or other structural data. In particular, it is not affected by the ordering of H atoms, and structures such as those of ices Ih and XI (the former being H-disordered and the latter H-ordered), with the same topology, will have the same sequence $\{C_n\}$. At present, there are five other known pairs of ice structures sharing the same topology, and related one to the other through an order/disorder phase transition. Then, one has six pairs of ice polymorphs: Ih-XI, III-IX, V-XIII, VI-XV, VII-VIII, and XII-XIV [7], where the first polymorph in each pair is H-disordered and the second is H-ordered. For our present purposes, we will only refer in the following to the disordered case, but understanding that it represents both members of the corresponding pair of ice polymorphs. In addition to these,

there exist other ice structures for which no pair has been found: ice Ic (H-disordered), ice II (H-ordered), and ice IV (H-disordered). Finally, ice X is topologically equivalent to ices VII and VIII, but with the important difference that in ice X hydrogen atoms lie midway between oxygen atoms, so that water molecules lose in fact their own entity (this is however unimportant for our present considerations). Thus, one has 9 topologically different ice structures. We note that the network associated to ice VII (as well as ices VIII and X) is composed of two interpenetrating but disjoint subnetworks, each of them equivalent to the ice Ic network. There is another case, the pair VI-XV, for which the network also consists of two disjoint subnetworks, but they are not equivalent to the network of any other known ice polymorph.

TABLE I: Crystal system and space group for the ice polymorphs considered in this work, along with the references from where crystallographic data were taken.

Phase	Crystal system	Space group	Ref.
Ih	Hexagonal	$P6_3/mmc$, 194	[60]
Ic	Cubic	$Fd\bar{3}m$, 227	[61]
II	Rhombohedral	$R\bar{3}$, 148	[62]
III	Tetragonal	$P4_12_12$, 92	[63]
IV	Rhombohedral	$R\bar{3}c$, 167	[64]
V	Monoclinic	$A2/a$, 15	[63]
VI	Tetragonal	$P4_2/nmc$, 137	[65]
VII	Cubic	$Pn\bar{3}m$, 224	[65]
XII	Tetragonal	$I\bar{4}2d$, 122	[66]

For the above reasons we will study here the ice polymorphs given in Table I, where we indicate the crystal system, space group, and the reference from where we took the crystal data to generate the corresponding supercells. In general, a study of the asymptotic behavior of the sequence $\{C_n\}$ for a given network requires the generation of large supercells. For the ice structures considered in this work, supercells including around 10^5 oxygen sites were generated. We have calculated the numbers $\{C_n\}$ of SAWs in such supercells by exact enumeration of the possible walks up to $n = 27$, using a backtracking algorithm [51].

III. RESULTS AND DISCUSSION

The mean numbers C_n of SAWs corresponding to different ice structures are presented in Table II for three walk lengths: $n = 5, 10$, and 15 . Note that in some cases C_n is not an integer number, since C_n^i corresponding to different starting sites i are different [see Eq. (1)]. We have checked that the sequence $\{C_n\}$ obtained for ice Ic coincides with that presented earlier for diamond up to

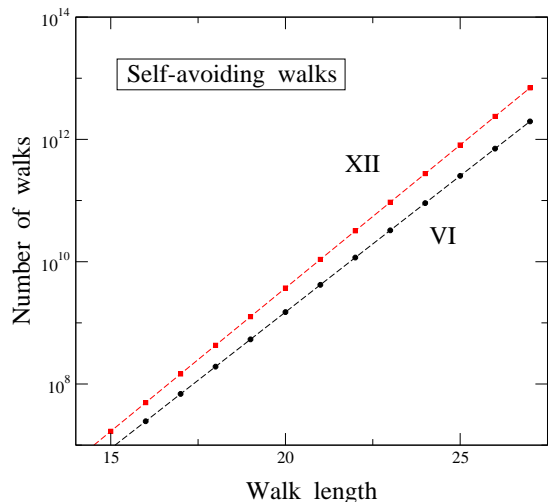


FIG. 2: Linear-log plot of the number of self-avoiding walks C_n on the structures of ice VI (circles) and XII (squares).

$n = 27$ [48, 49]. The number of walks C_n increases fast for rising n , as expected from the exponential part μ^n in Eq. (2) for $\mu > 1$. The increase in C_n as a function of the walk length n is shown in Fig. 2 for ices VI and XII, in a linear-logarithmic plot. Among the considered ice polymorphs, these two present the smallest and largest C_n values, respectively, and for other crystalline ice structures, C_n values lie between those of ices VI and XII. Comparing results for these two structures, we find a ratio $C_{27}(\text{XII})/C_{27}(\text{VI}) = 3.52$ for SAWs of length $n = 27$, the largest walks considered here. This ratio between C_n values of different structures increases as n is raised. In fact, according to Eq. (2), $C_n(\text{XII})/C_n(\text{VI})$ should increase for large n as $(\mu_{\text{XII}}/\mu_{\text{VI}})^n$. The dependence of $\log_{10} C_n$ on n shown in Fig. 2 is roughly linear, showing the leading contribution of the exponential term μ^n in Eq. (2). In general, for the structures under consideration, one expects

$$\log_{10} C_n - \log_{10} C_{n-1} = \log_{10} x_n \xrightarrow{n \rightarrow \infty} \log_{10} \mu \quad (6)$$

Thus, the slope of $\log_{10} C_n$ vs n shown in Fig. 2 converges for large n to $\log_{10} \mu$.

To obtain insight into the differences between C_n values for the different ice polymorphs, it is convenient to consider the topology of the corresponding crystal structures. Thus, given the variety of ice structures, it is not strange that some topological characteristics display clear differences between different polymorphs, as could be expected from the pressure/temperature range where they are stable. In this line, a first characteristic observable in the ice networks is the presence of loops (rings of water molecules), which define the particular topology of each structure. The statistics of rings in ice polymorphs has been considered in detail elsewhere [7, 22]. In particular, the mean ring size, $\langle L \rangle$, can be useful to connect topological and thermodynamic properties of these ice structures.

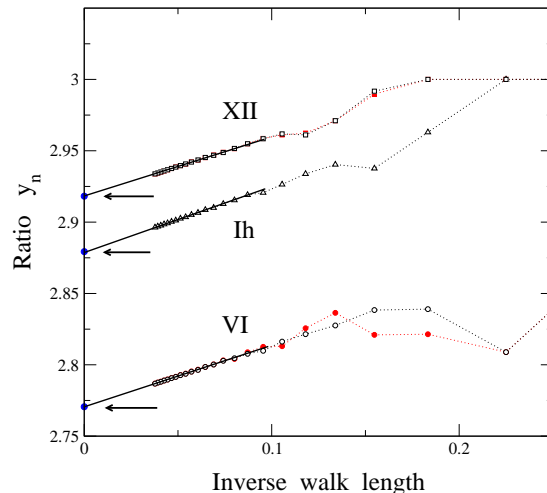


FIG. 3: Ratio y_n vs inverse walk length for ice VI (circles), Ih (triangles), and XII (squares). For ice VI and XII, results for two topologically different starting sites are shown (open and solid symbols), as derived from the corresponding sequence $\{C_n^i\}$. For each structure an arrow indicates the value of the connective constant μ obtained from an extrapolation of y_n for $1/n \rightarrow 0$.

In Table II we present $\langle L \rangle$ along with the minimum ring size L_{min} for the various polymorphs.

For a loop-free network (Bethe lattice or Cayley tree [52, 53]), the number of SAWs is given by

$$C_n^B = z(z-1)^{n-1} \quad (7)$$

where z is the number of nearest neighbors (degree or connectivity in the language of graph theory), assumed to be the same for all sites. For actual crystal structures, with networks including loops, C_n will be in general smaller than C_n^B , and for a given n the number of n -step SAWs is affected by the presence of rings of size $L \leq n$. For example, for our networks with $z = 4$ the maximum number C_5 of 5-step SAWs is that corresponding to the Bethe lattice: $C_5^B = 324$. Then, the lower values of C_5 for some ice networks (see Table II) are due to the presence of rings including five or less nodes. This happens for ices V and VI which contain four-membered rings ($L_{min} = 4$) and ice III with $L_{min} = 5$. For longer SAWs (larger n), loops with higher number of nodes also contribute to reduce the number C_n with respect to that of the Bethe lattice.

The connective constant μ has been obtained for the considered ice structures from the corresponding sequences $\{C_n\}$ by using the procedure described in Sect. II. In Fig. 3 we present the mean values y_n defined in Eq. (5) for three different structures (ices Ih, VI, and XII) as a function of the inverse walk length $1/n$. In fact, for ices VI and XII we show separately the values derived from the ratios C_{n+1}^i/C_n^i corresponding in each case to two topologically non-equivalent sites (open and solid symbols). Although results for those non-equivalent

TABLE II: Average number C_n of SAWs for walk length $n = 5, 10,$ and 15 , for different ice structures, along with the corresponding connective constant μ . Error bars of μ values are $\pm 2 \times 10^{-4}$. L_{min} and $\langle L \rangle$ are the minimum and mean ring size for each ice structure. a is the coefficient of the quadratic term in the coordination sequence, $N_k \sim ak^2$, as in Eq. (8). Data for ice VII are not given, since they coincide with those of ice Ic.

Network	C_5	C_{10}	C_{15}	μ	a	$\langle L \rangle$	L_{min}
Ih	324	70188	14776128	2.8793	2.62	6	6
Ic	324	70188	14774652	2.8792	2.50	6	6
II	324	73032	15996858	2.9049	3.50	8.52	6
III	317.3	68346.7	14156657.3	2.8714	3.24	6.67	5
IV	324	74241	16537432.5	2.9162	4.12	9.04	6
V	308.3	63877.4	12886447.7	2.8596	3.86	8.36	4
VI	284	51021.6	8855288.8	2.7706	2.00	6.57	4
XII	324	75245.3	16832260	2.9179	4.26	7.6	7
Square	284	44100	6416596	2.6382	0.0	4	4
Bethe	324	78732	19131876	3.0000	–	–	–

sites can be clearly different for small n values, for larger n they converge for each ice polymorph to the same limit. This should be expected, as for large length n , the walk loses memory of the starting node. The resulting values for the connective constant μ of the considered structures are given in Table II. We estimate for these μ values an error bar of $\pm 2 \times 10^{-4}$, due basically to the extrapolation $n \rightarrow \infty$. A check of our procedure is provided by the diamond structure, topologically equivalent to the ice Ic network, and for which the connective constant is known to be $\mu = 2.8790$ [45]. This value coincides within error bars with our result for ice Ic: $\mu = 2.8792(2)$. For comparison with results for the ice networks, note that for the loop-free Bethe lattice with $z = 4$, one has $\mu = 3$, as can be straightforwardly derived from Eq. (7). We also include in Table II the connective constant for the two-dimensional (2D) square lattice: $\mu = 2.6382$ [54] (also with $z = 4$).

As indicated above, the connective constant μ is a purely topological concept, and therefore should in some way be related with other (more basic) topological aspects of the ice structures. The first quantity to be compared with μ will be the mean loop size $\langle L \rangle$. In Fig. 4 we present the connective constant of various ice polymorphs vs $\langle L \rangle$. For the sake of comparison, we include a data point for the 2D square lattice, where all loops have $L = 4$. One first observes in this plot a tendency of the connective constant μ to increase for rising $\langle L \rangle$. There appears, however, an appreciable dispersion of the data points for different ice polymorphs, indicating a low correlation between both quantities. A more careful observation of the data shown in Fig. 4 reveals that the points corresponding to the ice structures are roughly aligned, with the exception of ices V and VI that appreciably de-

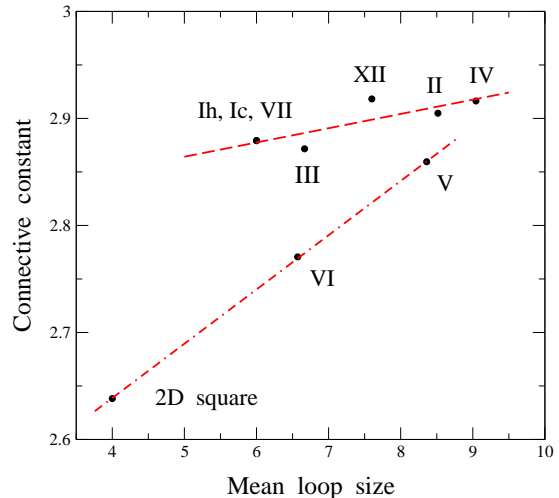


FIG. 4: Connective constant μ vs mean ring size $\langle L \rangle$ for crystalline ice structures. Labels indicate the ice structure corresponding to each data point. Ices Ih, Ic, and VII appear as a single point. The dashed-dotted line is a fit for the structures including four-membered rings (2D square lattice, ices V and VI). The dashed line is a least-square fit for the other ice structures.

part from the general trend. Common to these two ice polymorphs is that they are the only ones including four-membered rings ($L_{min} = 4$). In fact, one observes a good linear correlation between μ and the mean ring size $\langle L \rangle$ for these structures and the 2D square lattice (dashed-dotted line). The dashed line in Fig. 4 is a linear fit to the data points of ice structures not including four-

membered rings. For these structures we have $L_{min} > 4$, i.e., $L_{min} = 5$ for ice III, $L_{min} = 6$ for ices Ih, Ic, II, and IV, and $L_{min} = 7$ for ice XII. We observe in fact that the point corresponding to ice III lies below the dashed line, whereas that corresponding to ice XII appears above it. This is in line with the trend found for ices V and VI, since $L_{min}(\text{III}) < 6 < L_{min}(\text{XII})$.

From these results we conclude that the connective constant tends to increase as the ring mean size increases, but the presence of four-membered rings strongly affects the actual value of μ . Thus, the connective constant for ice VI is clearly lower than that of ice III, in spite of the fact that both polymorphs have very similar values for $\langle L \rangle$. This influence of four-membered rings decreases, however, for larger $\langle L \rangle$, as can be seen by comparing μ values for ices II and V.

As mentioned in the Introduction, the network topology can be characterized by the so-called coordination sequences $\{N_k\}$ ($k = 1, 2, \dots$), where N_k is the number of sites at a topological distance k from a reference site [22]. For 3D structures, N_k increases at large distances as:

$$N_k \sim a k^2 \quad , \quad (8)$$

where a is a network-dependent parameter. N_k increases quadratically with k just as the surface of a sphere increases quadratically with its radius. For structures including topologically non-equivalent sites, the actual coordination sequences corresponding to different sites may be different, but the coefficient a coincides for all sites in a given structure [22]. The parameter a can be used to define a ‘topological density’ for ice polymorphs, $\rho = w a$, where w is the number of disconnected subnetworks in the considered network [22]. Usually $w = 1$, but for ice structures including two interpenetrating networks (as ices VI and VII) one has $w = 2$.

In Fig. 5 we display the connective constant μ of ice polymorphs vs the coefficient a derived from the coordination sequences. As in Fig. 4, we also include a point for the 2D square lattice. We find again that μ increases for increasing parameter a , but there appears a dispersion in the data points, which can be associated to the minimum ring size of the considered ice structures. In particular, ice polymorphs including four-membered rings ($L_{min} = 4$) depart appreciably from the general trend of the other structures, similarly to the correlation between μ and the mean loop size $\langle L \rangle$ shown in Fig. 4. Then, we also present in Fig. 5 two different fits. On one side, the dashed-dotted line is a linear fit for the structures with $L_{min} = 4$, including the 2D square lattice. On the other side, the dashed line is a least-square fit for the ice polymorphs with $L_{min} > 5$, where all of them have $L_{min} = 6$ except ice XII, for which $L_{min} = 7$ (see Table II). For the remaining ice polymorph (ice III), with $L_{min} = 5$, the corresponding point (full square) lies on the region between both lines in Fig. 5.

One of the goals of the present work consists in finding relations between topological characteristics and thermo-

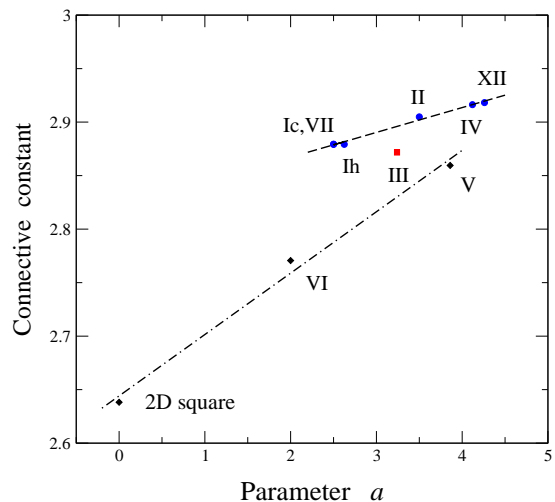


FIG. 5: Connective constant μ vs parameter a of coordination sequences for different ice polymorphs. Labels indicate the ice structure corresponding to each data point. Ices Ic and VII are represented by a single point, since they have the same coordination sequence (parameter a) and connective constant. The dashed-dotted line is a fit for the structures including four-membered rings (2D square lattice, ices V and VI). The dashed line is a least-square fit for ice polymorphs with minimum ring size $L_{min} > 5$.

dynamic properties of ice polymorphs. In this line, it has recently been shown that the network topology plays a role to quantitatively describe the configurational entropy associated to hydrogen disorder in ice structures [23]. This has been in fact known after the work by Nagle [55], who calculated the entropy for ices Ih and Ic. This author showed that the actual structure is relevant for this purpose, by comparing his results with Pauling’s value for the configurational entropy, derived in a simple approximation for a loop-free network (Bethe lattice). It has been recently shown that a simple procedure based on thermodynamic integration yields reliable results for the configurational entropy, s , of other ice structures with hydrogen disorder [23]. This method was applied to ice VI, for which an entropy per site $s = 0.4214(1)$ was found, vs $s = 0.4107(1)$ for ice Ih and Pauling’s value $s = 0.4055$ [56]. Note that s is dimensionless and can be converted to the physical configurational entropy S as $S = N k_B s$, with N the number of water molecules (nodes in the simplified network) and k_B Boltzmann’s constant. It thus appears that the topology of the network has a non-negligible influence on the entropy of the hydrogen distribution over the available lattice sites.

In Fig. 6 we present the configurational entropy per site vs the connective constant μ for ices Ih and VI, as well as for the Bethe lattice (Pauling result) and the 2D square lattice. The entropy value for the ice model on the square lattice has been taken from an exact calculation by Lieb [57]: $s = 0.4315$. One observes in this figure a negative correlation between the entropy s and μ . The

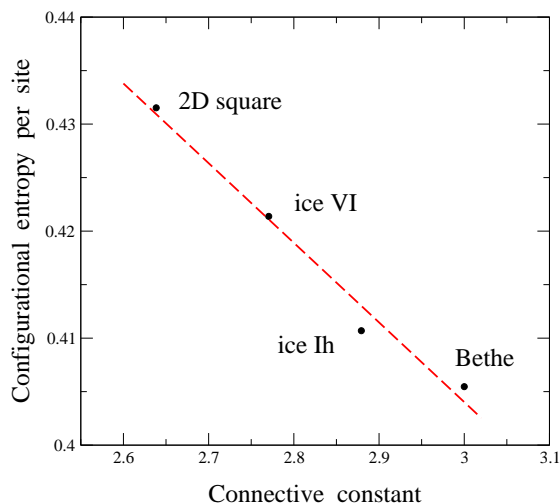


FIG. 6: Configurational entropy per site vs connective constant μ for various networks. The dashed line is a least-square fit to the data points.

dashed line is a least-square fit to the data points. We do not see any reason why this correlation should be linear, but it seems clear that there is a relation between both magnitudes. A qualitative argument for this relation is the following. The connective constant is a measure of the mean effective number of sites connected to a node in a long self-avoiding walk. For the distribution of hydrogen atoms on the links of the ice networks according to the Bernal-Fowler rules, a larger μ means an increase in the correlations in the occupancy of the available hydrogen sites, as information on the actual occupancy of a link propagates ‘more effectively’ through the ice network. Such an increase in the site-occupancy correlations causes a reduction in the number of available configurations compatible with the ice rules on a given structure, which translates into a decrease in the configurational entropy of the hydrogen distribution on the considered ice network. In this line, relations between SAWs and order/disorder problems, such as the Ising model on lattices, have been found and studied in the past [39, 58, 59].

Looking at Fig. 6 in more detail, one expects also that dimensionality can play a role in the actual values of the configurational entropy, and thus values derived for the 2D square lattice and the Bethe lattice (without a well defined dimension d ; for some purposes $d \rightarrow \infty$) may depart from the general trend found for 3D structures. This question should be investigated in the future, as con-

figurational entropy associated to hydrogen disorder can be precisely calculated for other crystalline ice structures using methods as those described in Refs. [23, 25].

IV. CONCLUSIONS

We have presented a calculation of self-avoiding walks on eight crystalline ice structures, which include all topologically different ice networks known so far. SAWs have been enumerated up to a walk length $n = 27$, which allowed us to obtain the connective constants for the different polymorphs. This parameter μ has turned out to be a quantitative topological characteristic of ice structures.

Correlations between the connective constant and other topological aspects of ice polymorphs have been found. The constant μ is in fact related with the mean ring size $\langle L \rangle$, although the correlation between both quantities is largely influenced by the minimum ring size L_{min} in each structure. A similar correlation between the connective constant and the parameter a controlling the coordination sequences in these crystalline structures ($N_k \sim ak^2$) has been found. This network-dependent parameter gives the topological density of ice polymorphs.

An interesting correlation has been found between the connective constant and the configurational entropy of hydrogen-disordered ice polymorphs. A larger μ favors stronger correlations in hydrogen occupancy of crystal sites, thus causing a decrease in the configurational entropy. This has been explicitly seen for ices Ih and VI, and compared to other networks with coordination number $z = 4$, such as the 2D square lattice and the Bethe lattice. A generalization to other crystalline ice polymorphs would be interesting, to check the extent to which this correlation is followed for this kind of structures. This will require a calculation of the configurational entropy for other hydrogen-disordered ice polymorphs, which is expected to change according to their topological characteristics.

Acknowledgments

R. Ramírez is thanked for inspiring discussions. This work was supported by Dirección General de Investigación (Spain) through Grant FIS2012-31713 and by Comunidad Autónoma de Madrid through Program MODELICO-CM/S2009ESP-1691.

-
- [1] V. F. Petrenko and R. W. Whitworth, *Physics of Ice* (Oxford University Press, New York, 1999).
 [2] A. N. Dunaeva, D. V. Antsyshkin, and O. L. Kuskov, *Solar System Research* **44**, 202 (2010).
 [3] T. Bartels-Rausch, V. Bergeron, J. H. E. Cartwright,

- R. Escribano, J. L. Finney, H. Grothe, P. J. Gutierrez, J. Haapala, W. F. Kuhs, J. B. C. Pettersson, et al., *Rev. Mod. Phys.* **84**, 885 (2012).
 [4] D. Eisenberg and W. Kauzmann, *The Structure and Properties of Water* (Oxford University Press, New York,

- 1969).
- [5] G. W. Robinson, S. B. Zhu, S. Singh, and M. W. Evans, *Water in Biology, Chemistry and Physics* (World Scientific, Singapore, 1996).
- [6] J. D. Bernal and R. H. Fowler, *J. Chem. Phys.* **1**, 515 (1933).
- [7] C. G. Salzmann, P. G. Radaelli, B. Slater, and J. L. Finney, *Phys. Chem. Chem. Phys.* **13**, 18468 (2011).
- [8] S. J. Singer and C. Knight, *Adv. Chem. Phys.* **147**, 1 (2012).
- [9] G. Malenkov, *J. Phys.: Condens. Matter* **21**, 283101 (2009).
- [10] W. B. Pearson, *The crystal chemistry and physics of metals and alloys* (Wiley, New York, 1972).
- [11] A. F. Wells, *Structural inorganic chemistry* (Clarendon Press, Oxford, 1986), 5th ed.
- [12] F. Liebau, *Structural chemistry of silicates: structure, bonding, and classification* (Springer, Berlin, 1985).
- [13] V. A. Blatov, *Acta Cryst. A* **56**, 178 (2000).
- [14] I. A. Baburin and V. A. Blatov, *Acta Cryst. B* **63**, 791 (2007).
- [15] C. Knight and S. J. Singer, *J. Chem. Phys.* **129**, 164513 (2008).
- [16] J. H. Conway and N. J. A. Sloane, *Proc. R. Soc. London A* **453**, 2369 (1997).
- [17] R. W. Grosse-Kunstleve, G. O. Brunner, and N. J. A. Sloane, *Acta Cryst. A* **52**, 879 (1996).
- [18] C. P. Herrero, *J. Chem. Soc.: Faraday Trans.* **90**, 2597 (1994).
- [19] J. G. Eon, *Acta Cryst. A* **58**, 47 (2002).
- [20] G. O. Brunner, *Zeolites* **13**, 88 (1993).
- [21] J. G. Eon, *Acta Cryst. A* **60**, 7 (2004).
- [22] C. P. Herrero and R. Ramírez, *Phys. Chem. Chem. Phys.* **15**, 16676 (2013).
- [23] C. P. Herrero and R. Ramírez, *Chem. Phys. Lett.* **568-569**, 70 (2013).
- [24] L. G. MacDowell, E. Sanz, C. Vega, and J. L. F. Abascal, *J. Chem. Phys.* **121**, 10145 (2004).
- [25] B. A. Berg, C. Muguruma, and Y. Okamoto, *Phys. Rev. B* **75**, 092202 (2007).
- [26] C. Domb, *Adv. Chem. Phys.* **15**, 229 (1969).
- [27] K. Binder and D. W. Heermann, *Monte Carlo Simulation in Statistical Physics* (Springer, Berlin, 1988).
- [28] I. Jensen, *J. Phys. A: Math. Gen.* **37**, 5503 (2004).
- [29] P. G. de Gennes, *Scaling Concepts in Polymer Physics* (Cornell Univ. Press, Ithaca, New York, 1979).
- [30] S. Caracciolo, B. M. Mognetti, and A. Pelissetto, *J. Chem. Phys.* **125**, 094904 (2006).
- [31] G. Rychlewski and S. G. Whittington, *J. Stat. Phys.* **145**, 661 (2011).
- [32] S. B. Lee, H. Nakanishi, and Y. Kim, *Phys. Rev. B* **39**, 9561 (1989).
- [33] E. J. J. V. Rensburg, *The Statistical Mechanics of Interacting Walks, Polygons, Animals and Vesicles* (Oxford Univ. Press, Oxford, 2000).
- [34] C. Vanderzande, *Lattice Models of Polymers* (Cambridge Univ. Press, Cambridge, 1998).
- [35] K. Kremer, A. Baumgartner, and K. Binder, *J. Phys. A: Math. Gen.* **15**, 2879 (1982).
- [36] K. Kremer and K. Binder, *Comp. Phys. Rep.* **7**, 259 (1988).
- [37] D. MacDonald, S. Joseph, D. L. Hunter, L. L. Moseley, N. Jan, and A. J. Guttmann, *J. Phys. A: Math. Gen.* **33**, 5973 (2000).
- [38] S. Caracciolo, A. J. Guttmann, I. Jensen, A. Pelissetto, A. N. Rogers, and A. D. Sokal, *J. Stat. Phys.* **120**, 1037 (2005).
- [39] C. P. Herrero, *J. Phys.: Condens. Matter* **7**, 8897 (1995).
- [40] C. P. Herrero and M. Saboyá, *Phys. Rev. E* **68**, 026106 (2003).
- [41] C. P. Herrero, *Phys. Rev. E* **71**, 016103 (2005).
- [42] T. Prellberg, *J. Phys. A: Math. Gen.* **34**, L599 (2001).
- [43] J. Krawczyk, T. Prellberg, A. L. Owczarek, and A. Rechnitzer, *Phys. Rev. Lett.* **96**, 240603 (2006).
- [44] V. Privman, P. C. Hohenberg, and A. Aharoni, in *Phase Transitions and Critical Phenomena*, edited by C. Domb and J. L. Lebowitz (Academic Press, London, 1991), vol. 14, pp. 1–134.
- [45] D. S. McKenzie, *Phys. Rep.* **27**, 35 (1976).
- [46] D. C. Rapaport, *J. Phys. A: Math. Gen.* **18**, 113 (1985).
- [47] S. Caracciolo, M. S. Causo, and A. Pelissetto, *Phys. Rev. E* **57**, R1215 (1998).
- [48] M. Chen and K. Y. Lin, *J. Phys. A: Math. Gen.* **35**, 1501 (2002).
- [49] A. J. Guttmann, *J. Phys. A: Math. Gen.* **22**, 2807 (1989).
- [50] A. J. Guttmann, in *Phase Transitions and Critical Phenomena*, edited by C. Domb and J. L. Lebowitz (Academic Press, London, 1989), vol. 13, pp. 1–234.
- [51] D. C. Rapaport, *Comp. Phys. Rep.* **5**, 265 (1987).
- [52] J. M. Ziman, *Models of disorder* (Cambridge University, Cambridge, 1979).
- [53] L. Stixrude and M. S. T. Bukowinski, *Am. Miner.* **75**, 1159 (1990).
- [54] A. J. Guttmann and A. R. Conway, *Ann. Comb.* **5**, 319 (2001).
- [55] J. F. Nagle, *J. Math. Phys.* **7**, 1484 (1966).
- [56] L. Pauling, *J. Am. Chem. Soc.* **57**, 2680 (1935).
- [57] E. H. Lieb, *Phys. Rev. Lett.* **18**, 692 (1967).
- [58] A. Pelissetto and E. Vicari, *Phys. Rep.* **368**, 549 (2002).
- [59] C. Domb, *J. Phys. C: Solid State Phys.* **3**, 256 (1970).
- [60] S. W. Peterson and H. A. Levy, *Acta Cryst.* **10**, 70 (1957).
- [61] H. König, *Z. Kristallogr.* **105**, 279 (1944).
- [62] B. Kamb, W. C. Hamilton, S. J. LaPlaca, and A. Prakash, *J. Chem. Phys.* **55**, 1934 (1971).
- [63] C. Lobban, J. L. Finney, and W. F. Kuhs, *J. Chem. Phys.* **112**, 7169 (2000).
- [64] H. Engelhardt and B. Kamb, *J. Chem. Phys.* **75**, 5887 (1981).
- [65] W. F. Kuhs, J. L. Finney, C. Vettier, and D. V. Bliss, *J. Chem. Phys.* **81**, 3612 (1984).
- [66] C. Lobban, J. L. Finney, and W. F. Kuhs, *Nature* **391**, 268 (1998).